

# **Supporting information**

## **A Polyoxometalate Supported Aminocatalyst for the Photo-catalytic Direct Synthesis of Imines from Alkenes and Amines**

Zhuolin Shi,<sup>†</sup> Jie Li,<sup>†</sup> Qiuxia Han,<sup>\*</sup> Xiaoyun Shi, Chen Si, Guiqin Niu, Pengtao Ma, Mingxue Li

Key Laboratory of Polyoxometalate Chemistry of Henan Province, School of Chemistry and Chemical Engineering, Henan University, Kaifeng, 475004, P. R. China

### **CONTENTS**

Section 1 Experimental Section

Section 2 Supplementary Structural Figures

Section 3 Characterizations of Catalysts.

Section 4 Catalysis Details

Section 5 References

## Section 1 Experimental Section

### 1. Measurement and Methods

The infrared (IR) spectra were recorded from a solid sample pelletized with KBr on a JASCO FT/IR-430. The powder X-ray diffractometry (PXRD) spectra were obtained on a Rigaku D/Max-2400. The vacuum inside the analysis chamber was maintained at  $1 \times 10^{-9}$  Pa during analysis. Thermogravimetric (TG) analysis was conducted on a Mettler-Toledo TGA/SDTA 851e instrument, with a heating rate of  $10\text{ }^{\circ}\text{C}\cdot\text{min}^{-1}$ , heated from 25 to  $1000\text{ }^{\circ}\text{C}$  under nitrogen. The diffuse reflectance UV-Vis absorption spectra were performed on a HITACHI UH4150 spectrophotometer (Japan). The morphology and structure of sample catalysts were characterized using a field-emission scanning electron microscope (SEM) (ZEISS, MERLIN Compact) at an accelerating voltage of 15.0 keV.  $^1\text{H}$  nuclear magnetic resonance (NMR) spectra were recorded on a Varian INOVA-400 MHz type ( $^1\text{H}$ , 400 MHz;  $^{13}\text{C}$ , 400 MHz) spectrometer. The chemical shifts are reported in ppm relative to  $\text{CDCl}_3$  ( $\delta=7.26$ ) for  $^1\text{H}$  NMR. ESR/EPR spectrum were detected on a Bruker a300. Mott-Schottky measurements were performed on an electrochemical workstation CHI 760E (Shanghai Chenhua Instrument Co., China). The working electrodes were prepared by dropping 80  $\mu\text{L}$  of slurry to the surface of indium-tin oxide (FTO) glass plates and covering approximately  $1\text{ cm}^2$ , Pt plate as the counter electrode and Ag/AgCl as reference electrode at frequencies of 1500, 2000, and 2500 Hz, respectively. 0.1 M of  $\text{Na}_2\text{SO}_4$  solution was used as the electrolyte. The photocatalytic reaction were performed on WATTCAS Parallel Light Reactor (WP-TEC-1020HSL) with 10W COB LED.

### 2. Synthesis.

All chemicals were of reagent grade quality obtained from commercial sources and used without further purification. L-N-tert-butoxy-carbonyl-2-(imidazole)-1-pyrrolidine (*L*-BCIP) is prepared according to the procedure reported by Luo et al <sup>1</sup>.  $\text{K}_4\text{PVW}_{11}\text{O}_{40}$  was obtained following the procedure reported by Domaille et al <sup>2</sup>. Above Prepared substance was characterized by IR and  $^1\text{H}$  NMR.

Synthesis of **ZnW-PYI**:  $\text{Zn}(\text{CH}_3\text{COO})_2\cdot 2\text{H}_2\text{O}$  (30.0mg, 0.164 mmol),  $\text{K}_4\text{PVW}_{11}\text{O}_{40}\cdot 2\text{H}_2\text{O}$  (27.6mg, 0.009 mmol), and *L*-BCIP (9.8 mg, 0.039 mmol) were added to a mixture of methanol (2 mL) and water (4 mL) and after stirring adjusted its pH value to 2.35 with  $1\text{ mol}\cdot\text{L}^{-1}$  HCl. The resulting admixture was sealed in a 25 mL Teflon-lined reactor and kept at  $110\text{ }^{\circ}\text{C}$  for 4 days. After cooling the autoclave to room temperature, washing the admixture with water and air-dried and then the white block crystals were obtained. (yield: 38%, based on  $\text{K}_4\text{PW}_{11}\text{VO}_{40}\cdot 2\text{H}_2\text{O}$ )

### 3. X-ray Crystallography

The suitable sample of **ZnW–PYI** was sealed in a glass tube and the information about X-ray diffraction degree were performed on a Bruker APEX-II CCD diffraction meter with the graphite-monochromated Mo K $\alpha$  radiation ( $\lambda = 0.71073$  Å) at 296(2) K. Lorentz and polarization rectification were utilized, and an applied multi-scan assimilation rectification was achieved with the SADABS scheme. Using Olex2, the framework of **ZnW–PYI** was detected by immediate ways (SHELXS-97) and Fourier syntheses improved with the SHELXL-2018/1 refinement package applying least-squares minimization algorithm.<sup>3,4</sup> In the last step, the non-hydrogen atoms there were refined anisotropically. The part of lattice water molecules were positioned by Fourier map. No hydrogen atoms associated with the water molecules got its position from Fourier map. All H atoms on water molecules were straightly incorporated in the structural formula. A conclusion of the crystal information and structure refinements are summarized in the following [Table 1](#).

**Table S1.** Crystal data and structure refinement for **ZnW–PYI**.

Crystal Data	<b>ZnW–PYI</b>
Empirical formula	C <sub>32</sub> H <sub>61</sub> N <sub>12</sub> Zn <sub>2</sub> P <sub>1</sub> W <sub>11</sub> O <sub>43</sub>
Formula weight	3485.91
Crystal system	Orthorhombic
Space group	<i>P</i> 2 <sub>1</sub> 2 <sub>1</sub> 2 <sub>1</sub>
<i>a</i> [Å]	13.5383(13)
<i>b</i> [Å]	19.5542(18)
<i>c</i> [Å]	26.470(2)
<i>V</i> [Å <sup>3</sup> ]	7007.5(11)
<i>Z</i>	4
$\rho_{\text{calcd}}$ [g·cm <sup>-3</sup> ]	3.296
$\mu$ [mm <sup>-1</sup> ]	18.766
data/parameters	3388/301
<i>F</i> (000)	6244.0
<i>R</i> <sub>int</sub>	0.0967
Flack	0.016(14)
2 $\Theta$ range for data collection/°	3.66 to 50.198
Index ranges	-14 $\leq$ <i>h</i> $\leq$ 16, -23 $\leq$ <i>k</i> $\leq$ 23, -17 $\leq$ <i>l</i> $\leq$ 31
Reflections collected	36831
Independent reflections	12469 [ <i>R</i> <sub>int</sub> = 0.0967, <i>R</i> <sub>sigma</sub> = 0.1132]
Data/restraints/parameters	12469/1394/910
GOF	0.990
<i>R</i> <sub>1</sub> <sup>a</sup> , <i>wR</i> <sub>2</sub> <sup>b</sup> [ <i>I</i> > 2 $\sigma$ ( <i>I</i> )]	0.0505, 0.0938
<i>R</i> <sub>1</sub> , <i>wR</i> <sub>2</sub> [all data]	0.0738, 0.1045
diff peak and hole, eÅ <sup>-3</sup>	1.45/ -1.70

[a]  $R_1 = \sum ||F_o| - |F_c|| / \sum |F_o|$ , [b]  $wR_2 = [\sum w(F_o^2 - F_c^2)^2 / \sum w(F_o^2)^2]^{1/2}$ ;  $w = 1/[\sigma^2(F_o^2) + (xP)^2 + yP]$ ,  $P = (F_o^2 + 2F_c^2)/3$ , where  $x = 0.0258$ ,  $y = 0$  for **ZnW–PYI**.

**Table S2.** The selected bond lengths of **ZnW–PYI**.

Bond	Length	Bond	Length
W(1)–O(35)	1.7219(19)	Zn(1)–O(17)	1.999(19)
W(1)–O(26)	1.795(19)	Zn(1)–O(14)	2.00(2)
W(1)–O(7)	1.881(18)	Zn(1)–N(10)	2.01(3)
W(1)–O(2)	1.938(19)	Zn(1)–O(29)	2.09(2)
W(1)–O(3)	1.977(19)	Zn(1)–O(25)	2.38(2)
W(1)–O(18)	2.339(19)	Zn(1)–O(20)	2.09(2)
P(1)–O(8)	1.5965(18)	Zn(2)–N(7)	1.94(3)
P(1)–O(25)	1.64(2)	Zn(2)–N(4)	2.01(2)
P(1)–O(1)	1.585(19)	Zn(2)–N(1)	2.05(2)
P(1)–O(18)	1.6272(18)	Zn(2)–O(35)	2.20(2)
		Zn(2)–O(30A)	2.25(2)

A: -1/2+X,7/2-Y,3-Z

The total BVS values of all oxygen atoms in ZnW-PYI suggests three protons are localized or delocalized in  $[\text{PW}_{11}\text{O}_{39}\text{Zn}(\text{PYI})]^{5-}$  anion units (Table S3).

**Table S3.** The bond valence sum (BVS) of all oxygen atoms in  $[\text{PW}_{11}\text{O}_{39}\text{Zn}(\text{PYI})]^{5-}$  anion.<sup>5</sup>

Atom	BVS	Atom	BVS	Atom	BVS
O1	1.979	O14	1.897	O27	1.990
O2	2.015	O15	1.881	O28	2.002
O3	1.900	O16	2.084	O29	1.724
O4	1.844	O17	1.950	O30	2.000
O5	2.024	O18	1.920	O31	1.798
O6	1.897	O19	1.847	O32	1.703
O7	2.091	O20	1.800	O33	1.842
O8	1.945	O21	1.827	O34	1.904
O9	2.051	O22	2.057	O35	1.969
O10	1.872	O23	1.605	O36	1.886
O11	2.066	O24	1.929	O37	1.803
O12	1.953	O25	1.848	O38	1.882
O13	1.698	O26	1.965	O39	1.798

## Section 2 Supplementary Structure Figures and Characterization

Elemental analyses, IR and powder X-ray diffraction (PXRD) and scanning electron microscope (SEM) indicated a pure phase for the bulk sample (Figure S1–3).

**Figure S1.** PXRD pattern of **ZnW–PYI**.

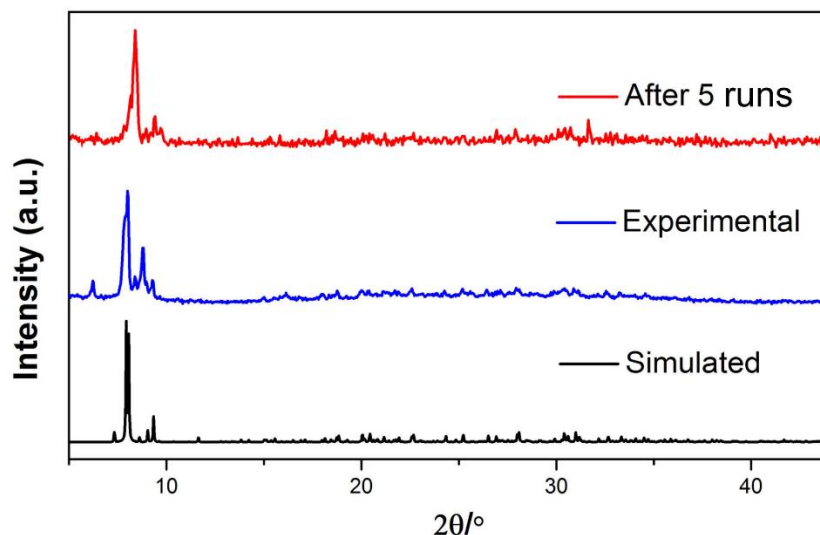
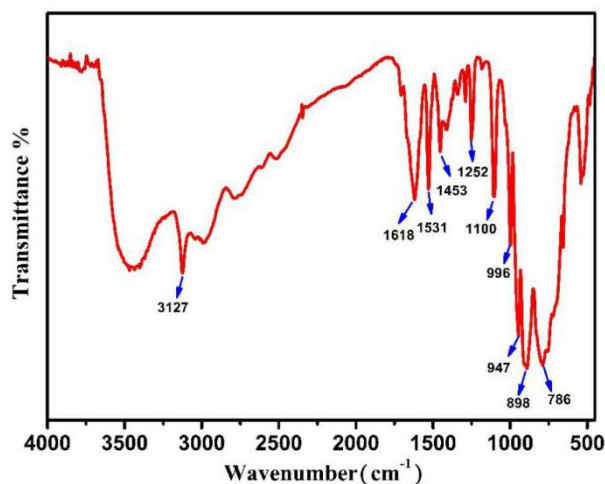
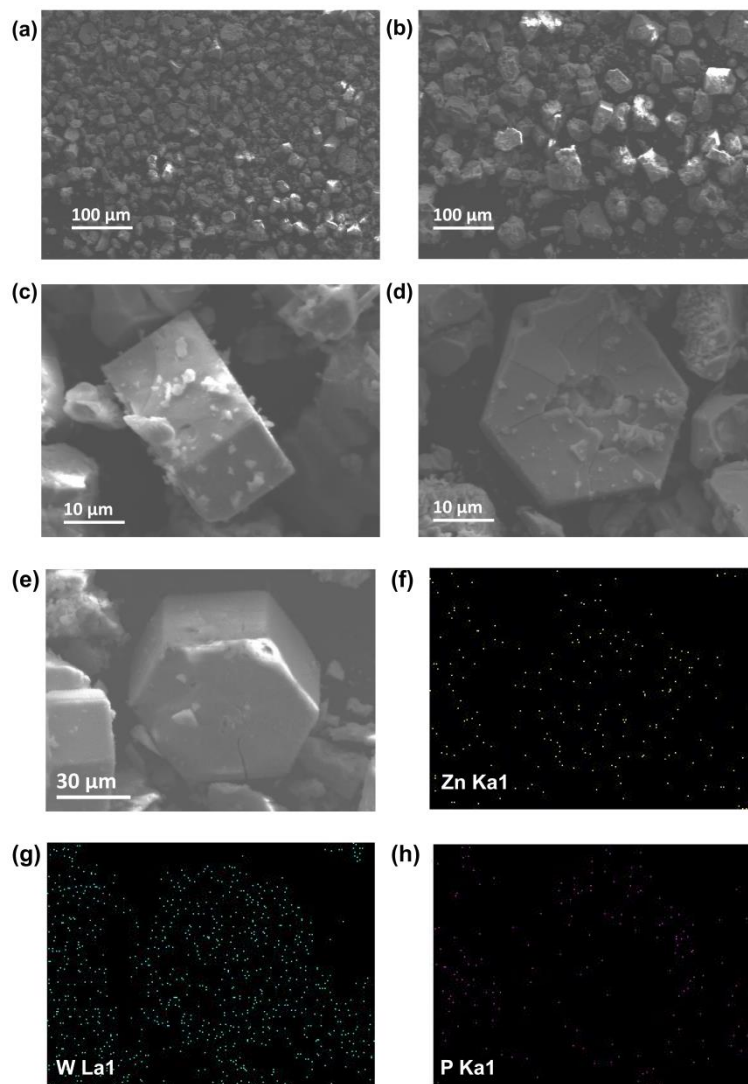


**Figure S2.** The IR spectra of **ZnW–PYI**.



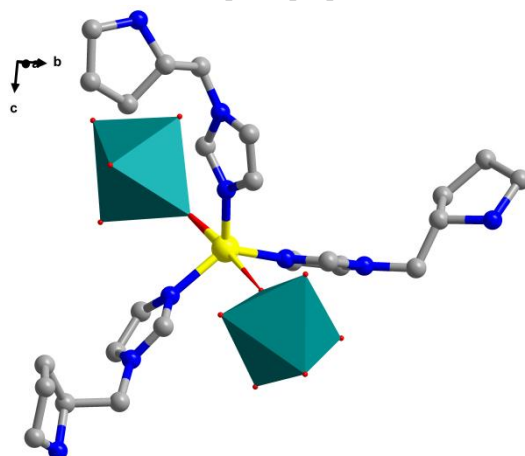
The IR spectra of **ZnW–PYI** are collected and shown the characteristic bands of  $\nu(\text{W-Od})$ ,  $\nu(\text{W-Oa})$ ,  $\nu(\text{W-Ob})$  and  $\nu(\text{W-Oc})$  vibrations in **ZnW–PYI** are in the ranges of 996 and 786  $\text{cm}^{-1}$ . The resonances at 1618 and 1252  $\text{cm}^{-1}$  are assigned to the (C-N) and (C-H) stretching vibrations of *L*-PYI, respectively. These characteristic vibration resonances confirm the existence of *L*-PYI ligands and  $[\text{PW}_{11}\text{ZnO}_{39}]^{5-}$  in **ZnW–PYI**. The results of the IR spectra are quite consistent with those of X-ray diffraction.

**Figure S3.** (a-d) SEM images displaying the morphology of **ZnW-PYI**. (e-h) EDS images with elements distribution of Zn (Ka), Mo (La) and P (Ka) in **ZnW-PYI**.



The morphology of **ZnW-PYI** sample was characterized by a scanning electron microscope (SEM) and showed hexagonal shaped blocks with smooth surfaces. Moreover, the energy dispersive spectroscopy (EDS) presented the specific distribution of individual elements in same block of sample. The different color intensities were assumed to be proportional to the metal composition in the same block of sample<sup>6</sup>, W (sky blue), P (Pink) and Zn (yellow) collected by elemental mapping, which indicated both W and Zn elements were homogeneously distributed in the framework of **ZnW-PYI**.

**Figure S4** Ball and stick representation of the concrete coordination environment of Zn(II) in compound **ZnW–PYI**, which is similar to a shape of propeller.



As shown in Fig. S4, the Zn(2) atom is five-coordinated with a distorted trigonal bipyramid geometry coordinated with three nitrogen atoms from three PYI ligands forming the equatorial plane and two terminal oxygen atoms from the two  $[\text{PZnW}_{11}\text{O}_{39}]^{5-}$  units occupying the axial positions (Color code: Zn(2), yellow spheres; N, blue spheres; O, red spheres; C, gray; W, teal polyhedron).

**Figure S5** N-H $\cdots$ O Hydrogen bonds (aqua line) interactions between protonated pyrrolidine rings and the POMs and ligands in **ZnW–PYI**.

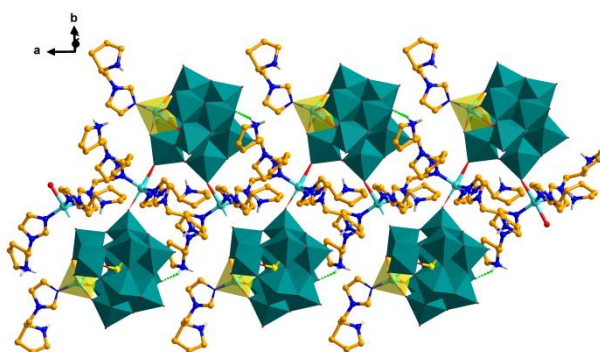


**Figure S6** The 2D network of **ZnW–PYI** showing the stack mode between POMs and ligands linking by hydrogen bonds, viewed along the b-axis.

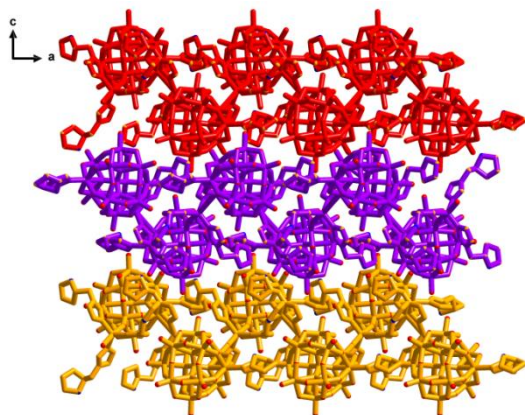
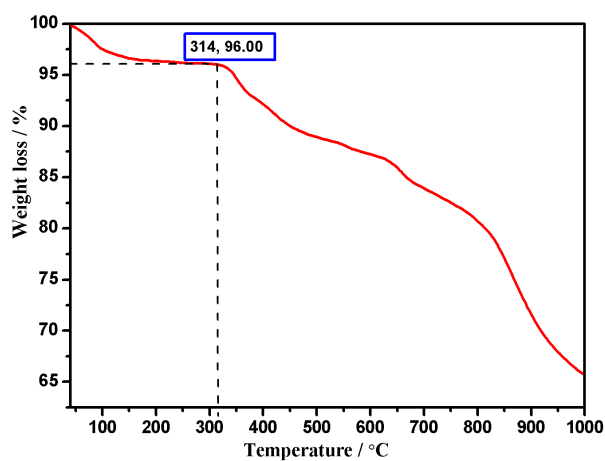




**Figure S7.** The thermogravimetric analysis of **ZnW–PYI**.



The thermal behavior of **ZnW–PYI** has been investigated under nitrogen atmospheres between 25~1000 °C by thermogravimetric analysis (TGA). The TG curve showed that **ZnW–PYI** gradually lose the guest water molecules in the temperature range 40~200 °C and the frameworks are stable up to ~314 °C. **ZnW–PYI** is not sensitive to air and moisture and can be stored at room temperature for months. **ZnW–PYI** exhibits a high chemical and thermal stability, which satisfies most of the prerequisites for an ideal platform for heterogeneous catalysis.

**Figure S8.** The estimated energy band gap of **ZnW–PYI** by the UV-Vis DRS based on the Kubelka-Munk Function.

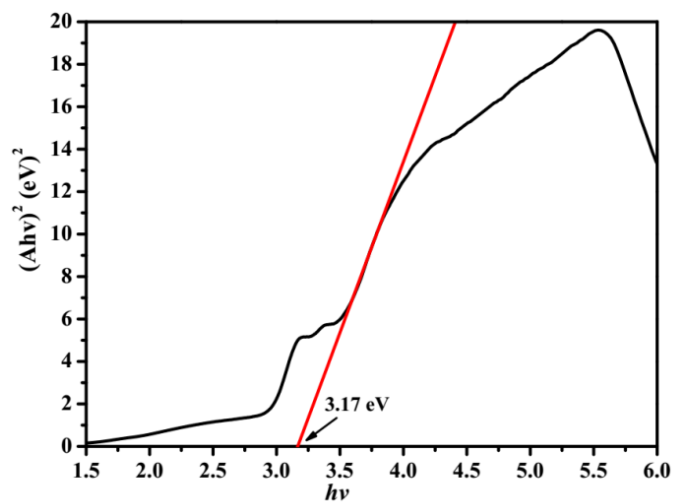
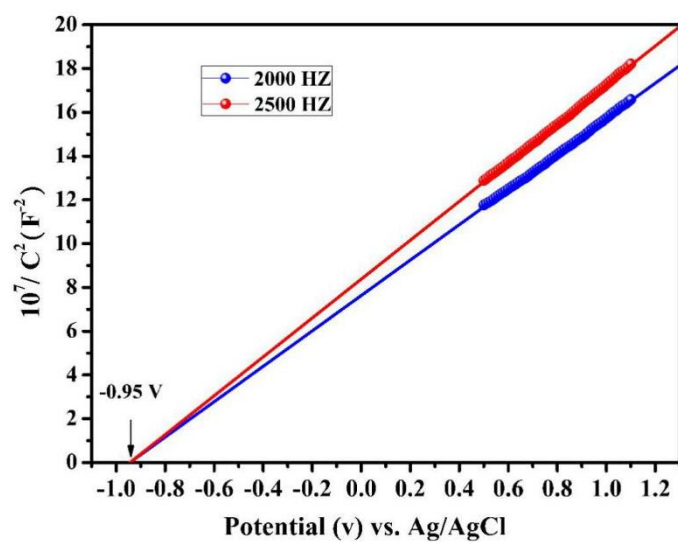
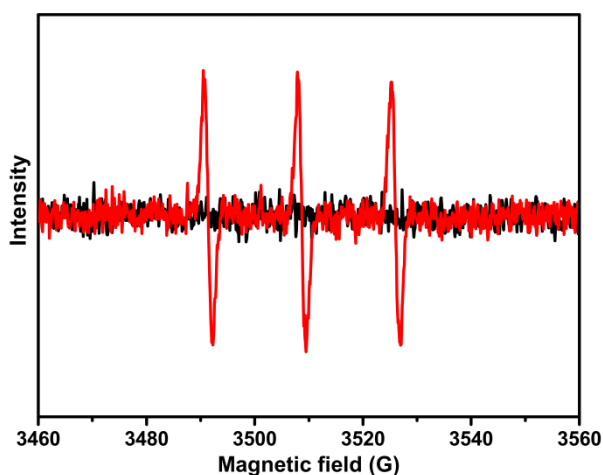


**Figure S9.** The Mott–Schottky plots of  $(\text{TBA})_3[\text{PW}_{12}\text{O}_{40}]$ .



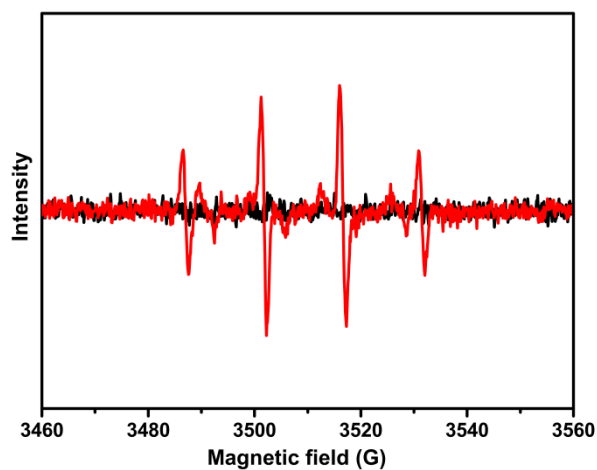
The Mott–Schottky measurements on  $(\text{TBA})_3[\text{PW}_{12}\text{O}_{40}]$  were performed at a frequency of 2000 and 2500 Hz, showing the LUMO level ( $-0.75\text{V}$  vs. NHE).

**Figure S10.** The EPR measurement of  $^1\text{O}_2$ .



The EPR that employing 2,2,6,6-tetramethylpiperidine (TEMP) as the typical spin-trapping agent for  $^1\text{O}_2$  revealed that active oxygen species was involved in the photo-oxidative coupling reaction of benzylamine.

**Figure S11.** The EPR measurement of  $\cdot\text{OH}$ .



The EPR using potassium monopersulfate triple salt (PMS)/DMPO as a hydroxyl radical ( $\cdot\text{OH}$ ) probe detected the formation of  $\cdot\text{OH}$  revealed that active oxygen species was involved in the photo-oxidative coupling reaction of benzylamine.

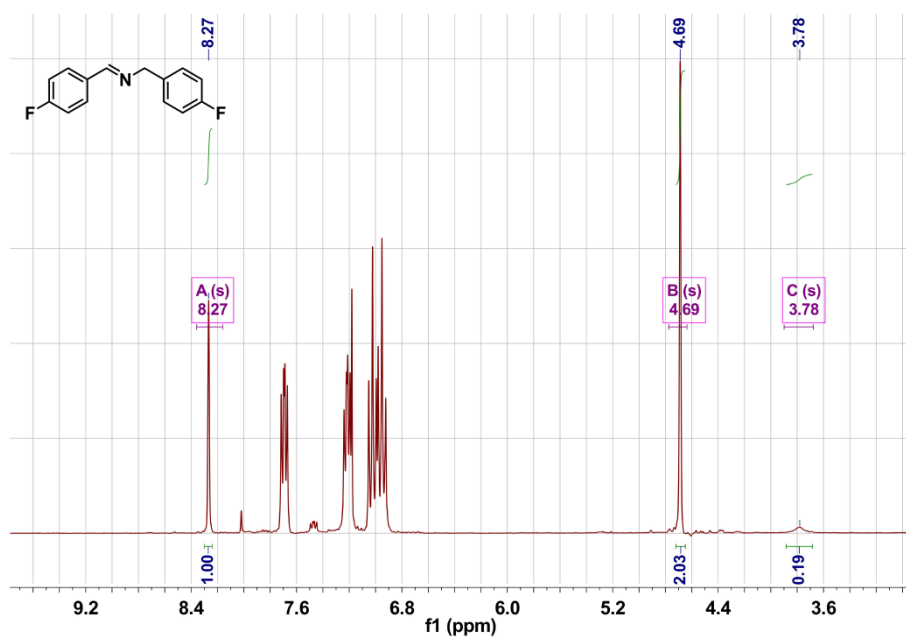
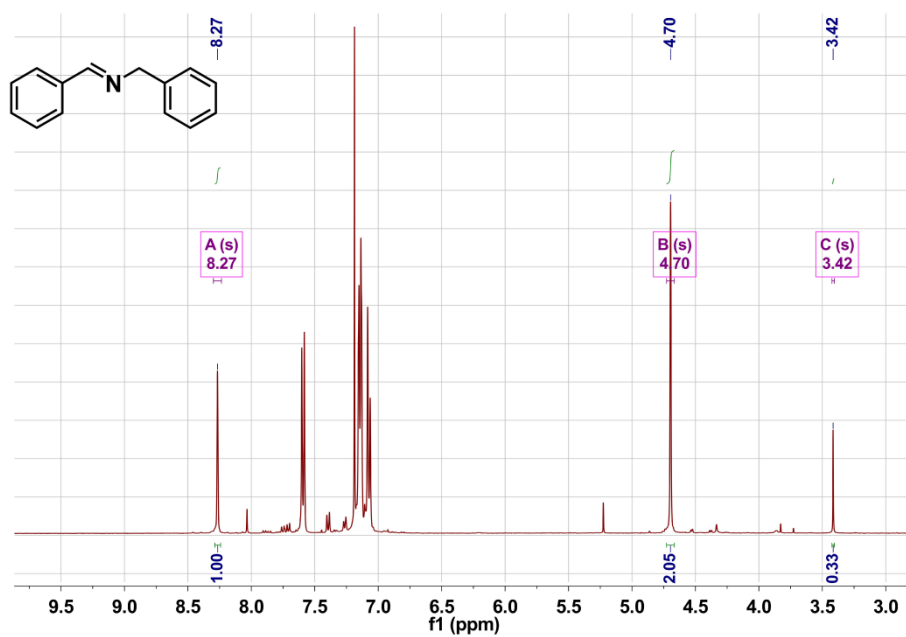
## Section 4 Catalysis details

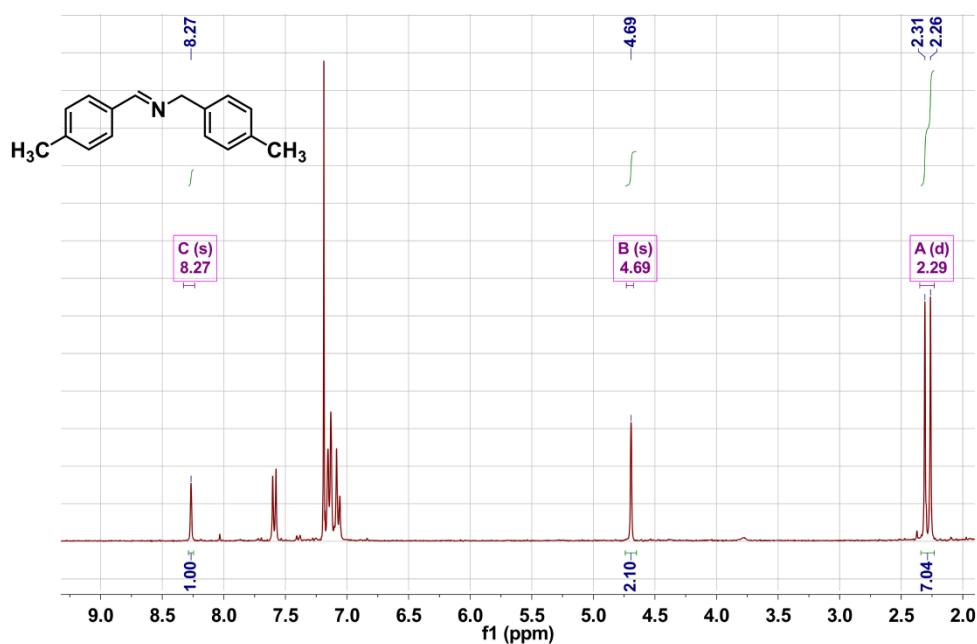
### 1. Typical procedure for the Oxidative self-Coupling of Amines.

Catalyst (10.0 mg, 2.925  $\mu\text{mol}$ , 0.29%), amine (1 mmol), acetonitrile (0.5 mL) was added to A glass tub, and then the tub was filled with oxygen and sealed. The mixture was exposed to a 10 W white LED lamp and stirred to react under room temperature. After reaction for 16 h, the catalyst was separate from the reaction solution by filtering, and the remaining mixture was dried in vacuo. Finally, the yield of the product is obtained by analysis corresponding  $^1\text{H}$  NMR spectrum.



## 2. $^1\text{H}$ NMR for Oxidative Self-coupling of Amines in $\text{CDCl}_3$ .

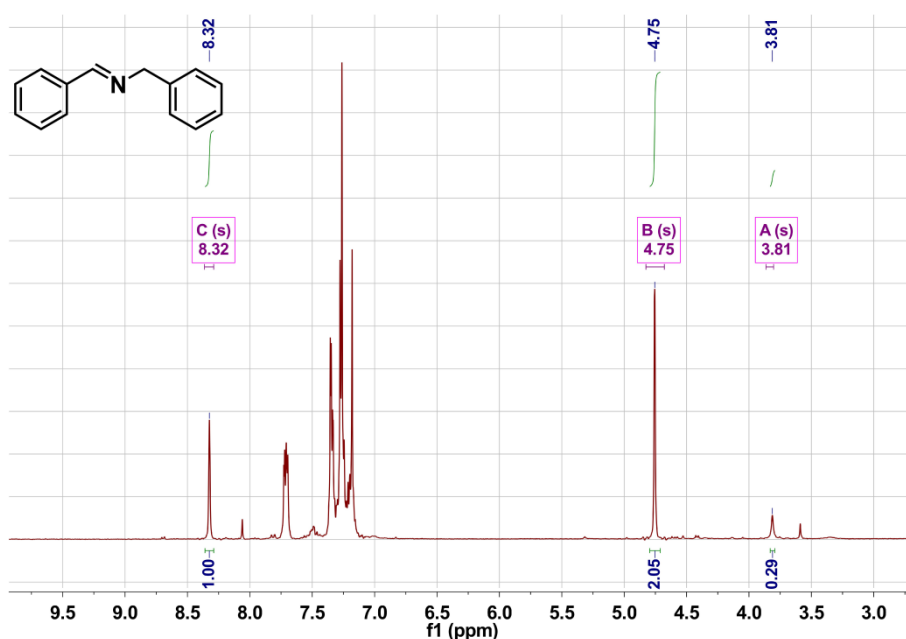


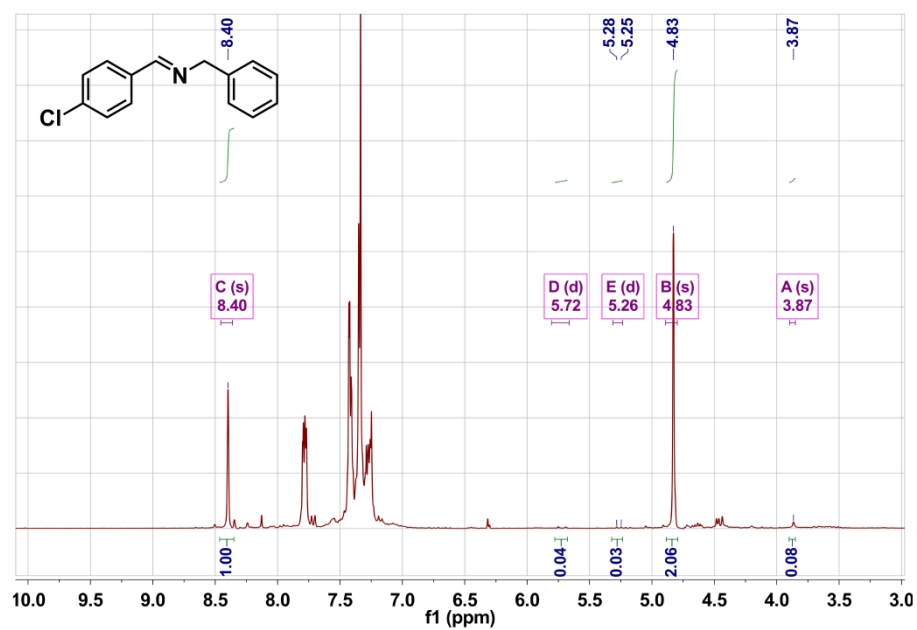
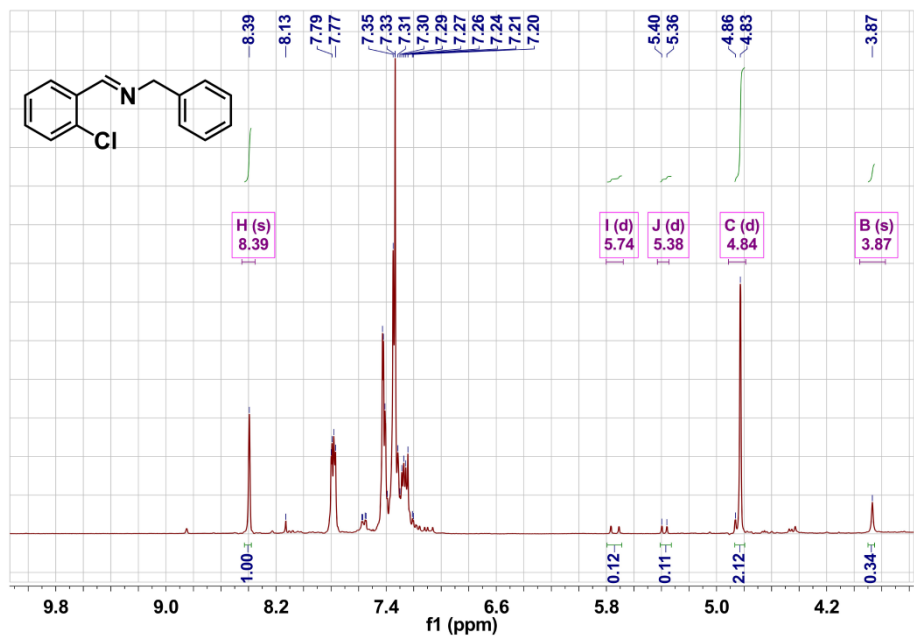


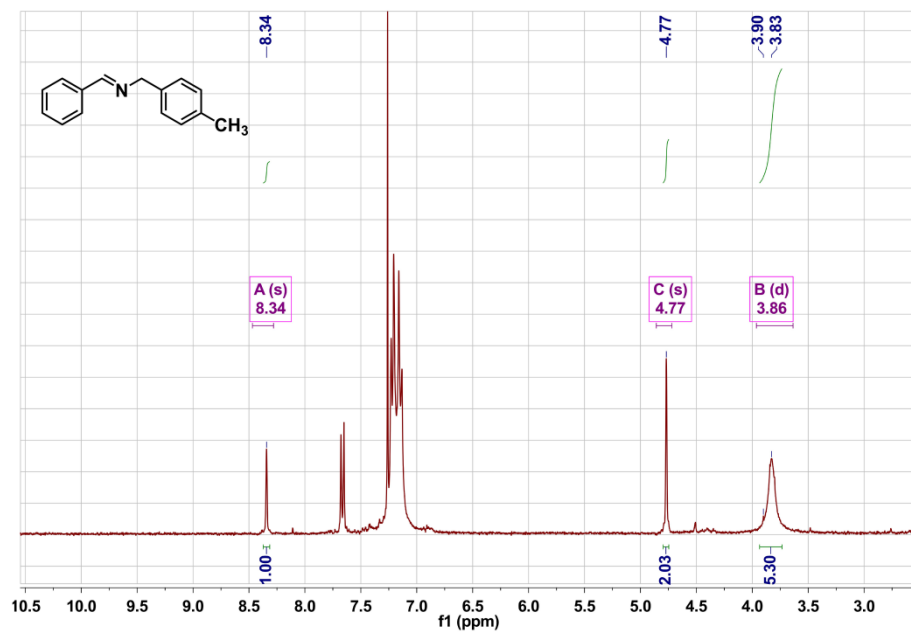
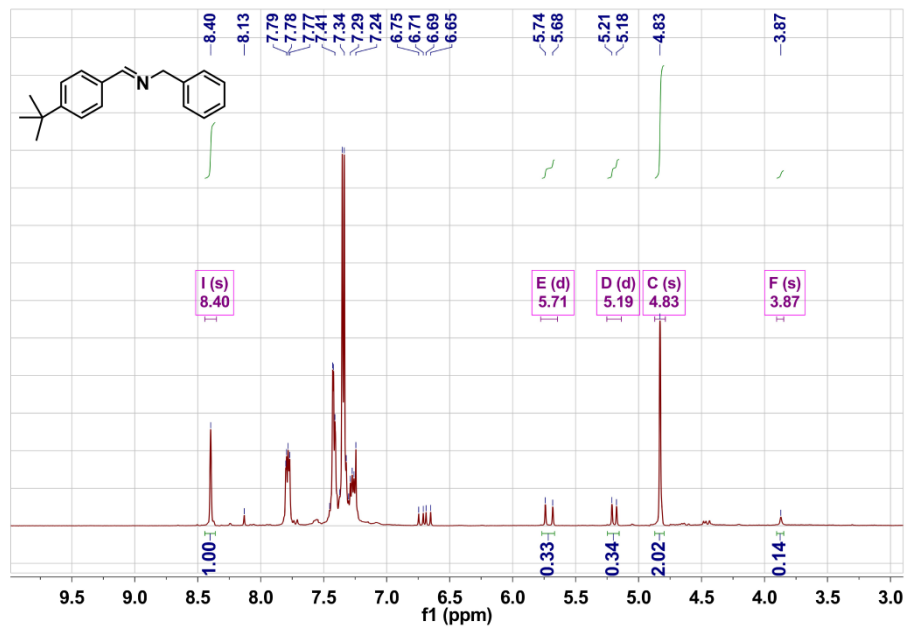
### 3. Typical Procedure for the Oxidative Coupling of Amines and Styrene.

Catalyst (10.0 mg 2.925  $\mu\text{mol}$ , 0.066%), amine (2.5 mmol), styrene (2.2 mmol), acetonitrile (0.5 mL) was added to a glass tub, and then the tub was filled with oxygen and sealed. The mixture was exposed to a 10 W white LED lamp and stirred to react under room temperature. After reaction for 16 h, the catalyst was separate from the reaction solution by filtering, and the remaining mixture was dried in vacuo. Finally, the yield of the product is obtained by analysis the corresponding  $^1\text{H}$  NMR spectrum.

### 4. $^1\text{H}$ NMR for the Oxidative Coupling of Amines and Styrene in $\text{CDCl}_3$ .



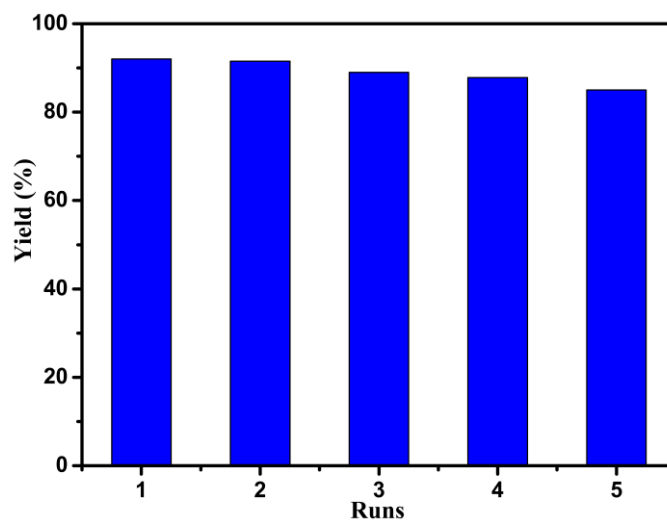






## 5. Recyclability of Oxidative Self-coupling of Amines for ZnW–PYI catalyst.

**Figure S12.** The recyclability test for the oxidative self-coupling of benzylamine



The recyclability test was executed for the oxidative self-coupling of benzylamine as model catalysis with 0.5 MPa O<sub>2</sub> under 365 nm light. The catalyst could be reused at least five times with moderate loss of activity from 92 to 85% yield. After every run, the catalyst was separated and accumulated by centrifugal separation followed by washing three times with methanol. The PXRD patterns of the initial and recovered samples after five cycles also further indicate the high stability of this catalyst (Figure S1b).

## Section 5 References.

1. Luo, S.; Mi, X.; Zhang, L.; Liu, S.; Xu, H.; Cheng, J. P. Functionalized Chiral Ionic Liquids as Highly Efficient Asymmetric Organocatalysts for Michael Addition to Nitroolefins. *Angew. Chem. Int. Ed.* **2006**, *45*, 3093.
2. Domaille, P. J. *J. Am. Chem. Soc.* **1984**, *106*, 7677.
3. Sheldrick, G. M. *Acta Crystallogr., Sect. C: Struct. Chem.*, **2015**, *C71*, 3–8.
4. Spek, A. L. *Acta Crystallogr., Sect. C: Struct. Chem.*, **2015**, *C71*, 9–18.
5. Brown, I.; Altermatt, D. D. *Acta Crystallogr. Sect. B*, **1985**, *41*, 244–247.
6. Huang C, Liu R, Yang W, et al. *Inorg. Chem. Front.* **2018**, *5*, 1923.